DOI: 10.1002/ejic.200500906

Design, Crystal Growth, Characterization, and Second-Order Nonlinear Optical Properties of Two New Three-Dimensional Coordination Polymers Containing Selenocyanate Ligands

Sheng-Li Li,[a,b] Jie-Ying Wu,[a] Yu-Peng Tian,*[a,c,d] Hai Ming,[b] Pei Wang,[b] Min-Hua Jiang,[c] and Hoong-Kun Fun[e]

Keywords: Self-assembly / Coordination polymer / Crystal growth / Nonlinear optical properties

Two new second-order nonlinear optical coordination polymers, zinc cadmium tetraselenocyanate ($[ZnCd(SeCN)_4]_n$, **1**) and cadmium mercury tetraselenocyanate ($[CdHg(SeCN)_4]_n$, **2**), have been synthesized by reactions of self-assembly. Their structural, optical, and physicochemical properties were characterized by X-ray diffraction, infrared and Raman spectroscopy, electronic spectra, and thermal analyses. Structure analyses reveal that they belong to the tetragonal system $I\bar{4}$ space group. The cell dimensions for **1**: a = 11.3420(1), b = 11.3420(1), c = 4.6326(1) Å, V = 595.94(1) Å^3, Z = 2, D_c = 3.331 g·cm^{-3}, R_1 = 0.0411, wR_2 = 0.1058; for **2**: a = 11.6579(7), b = 11.6579(7), c = 4.5109(4) Å, V = 613.06(8) Å^3, Z = 2, D_c = 3.970 g·cm^{-3}, R_1 = 0.0432, wR_2 = 0.1031. The structural features of **1** and **2** are Cd–Se=C=N–Zn and Hg–Se=C=N–Cd bridges, respectively, which lead to the formation of an infinite three-dimensional (3D) network. Consistent with their polar structures, compounds **1** and **2** exhibit powder second harmonic generation (SHG) responses much stronger than urea, indicating quite a promising application potential as useful nonlinear optical (NLO) materials.

Introduction

It is well known that the rapidly developing area of research on supramolecular architectures has provided implications for the rational design of functional materials[1,2] and a number of the assemblies are predominantly controlled by the coordination preferences of the transition metal and the ligand building blocks.[3,4] Recent developments in the specific, efficient syntheses by self-assembly processes of coordination complexes have afforded a variety of unusual topologies such as molecular helicates, grids, ladders, rings, and boxes.[5,6] Self-assembly of polynuclear structure has received considerable attention from researchers in areas ranging from chemistry to solid-state physics and biology.[7] Some complexes are of interest not only for their unusual structures and the simple synthetic methods used to prepare them, but also because they allow the preparation of polynuclear complexes in which several potentially interesting metal centers are designed to link in a well-defined spatial array. The use of metal complexes to function as molecular devices is one of the major interests in coordination chemistry.

There has been considerable interest in the synthesis of new materials with optical nonlinearities because of their potential use in device applications in telecommunications, optical computing, optical storage, and optical information processing. However, organic systems can suffer from problems such as volatility, low thermal stability, and mechanical weakness. The low-energy d–d transitions present in nearly all organometallic compounds, normally observed in the visible light region, will limit the usefulness of these materials. On the other hand, the inorganic ligands such as the ambidentate thiocyanate (SCN^-) and the selenocyanate ($SeCN^-$) ligand, can govern the nonlinearities for the metal complexes from the viewpoint of molecular design.[8] In particular, the group IIB divalent d^{10} ions, Zn^{2+}, Cd^{2+}, and Hg^{2+} complexes, have attracted our interest for their unique characteristics of pale color and high thermal stability.[9]

As a result of the unsymmetrical nature of complexes, optical activity can occur as specific physical effects such as nonlinear optical (NLO) response.[10] The incorporation of the strong conjugation ligands, such as the asymmetric selenocyanate (SeCN) groups in the title polymers with a three-dimensional (3D) network, can introduce strong electronic asymmetry and electron delocalization in the whole unsym-

[a] Department of Chemistry, Anhui University,
Hefei 230039, P. R. China
Fax: +86-551-5107342
E-mail: lsl1968@ahu.edu.cn
yptian@ahu.edu.cn
[b] Department of Physics, University of Science and Technology of China,
Hefei 230026, P. R. China
[c] State Key Laboratory of Crystal Materials, Shandong University,
Jinan 250100, P. R. China
[d] State Key Laboratory of Coordination Chemistry, Nanjing University,
Nanjing 210093, P. R. China
[e] X-ray Crystallography Unit, School of Physics, University Sains Malaysia,
11800 USM, Penang, Malaysia

metrical structure, resulting in large second-order microscopic and macroscopic nonlinearity. Considering this, attention has been paid to the following facts: (1) The large nonlinear optical response comes with a big conjugation system, which is able to provide sufficient electronic channels for the photoelectric process. (2) The electronic nature of the metal center has an influential effect on the nonlinear optical interactions. In particular, the d orbital of the transition metal can become a component of the π conjugation system, thus extending the electronic interactions; (3) Reducing the molecular symmetry can help the formation of a noncentrosymmetric space group. Then, specific crystallization techniques are taken into account to form a proper crystal lattice, in which the good microscopic NLO response can be collected rather than eliminated; (4) Making use of the coordination bond or forming the polymeric complex to connect molecules and sequentially control the alignment of molecules in the crystal, the interaction for the bulk NLO response could be accumulated.

As far as we know, the preparation of selenocyanate-containing metal–inorganic compounds along with their characterization have been reported, but the NLO properties of the selenocyanate-containing polymers have scarcely been described hitherto. Referring to the title NLO polymers, we have systemically carried out research[11] not only on the preparation, crystal growth, physicochemical, and nonlinear optical properties of the complexes, but also on the design and structure–property relationship, which is original and different from other related reports.[12] In the crystal growth process, we used a one-step building-block approach capable of forming a chemically stable system, which enabled us to grow the high-quality and transparent polymeric single crystals, in contrast to the complicated approach used before resulting in mixtures of small molecular compounds or perhaps even monomers. In this context, the building-block approach of self-assembly for the synthesis of coordination polymers illustrates both the importance of metal-ion geometry and the effect that the ligand backbone can have on network construction. This article deals with two novel 3D coordination polymers, $[ZnCd(SeCN)_4]_n$ (**1**) and $[CdHg(SeCN)_4]_n$ (**2**), and their preparation, crystal growth, structures, and NLO properties are described.

Results and Discussion

Single-Crystal Growth

The chalcogenocyanate ion, $SeCN^-$, is a linear triatomic pseudohalide and a highly versatile ambidentate ligand with a polarizable π system. It can coordinate to transition-metal ions through either the hard nitrogen or the soft selenium atom, or both, giving rise to linkage isomers or polymers.

The crystal growth processes of **1** and **2** were carried out in one step by self-assembling in aqueous solutions containing cadmium chloride, potassium selenocyanate, and zinc chloride (for **1**) or mercury chloride (for **2**). Preparations were accomplished by two continuous reactions, where M = Zn or Hg:

$$4\ KSeCN + MCl_2 = K_2M(SeCN)_4 + 2\ KCl$$

$$K_2M(SeCN)_4 + CdCl_2 = MCd(SeCN)_4 + 2\ KCl$$

We have obtained good single crystals from RMS and the experiments showed that the success of growing large and high-quality single crystals with low defect density was highly dependent on the purity of the starting materials. Several foreign metallic cations, such as Al^{3+}, Fe^{3+}, Co^{2+}, Ni^{2+}, Cu^{2+} and so forth, would badly influence the quality of the crystals, especially their transparency. Meanwhile, the crystal growth processes of the two polymers were affected by the pH value of RMS. We optimized the pH values of **1** and **2** solutions at 3.5–5.0 to get well-developed and transparent single crystals. As potassium selenocyanate (KSeCN) easily decomposes in air, the entire crystallization process was performed in a desiccator in vacuo. Moreover, the experiments indicated that the colors of **1** and **2** solutions easily turn slightly red or gray when the precipitates form as byproducts at a relatively high temperature, although the crystals show no decomposition and hygroscopic effect at atmospheric pressure and room temperature.

IR and Raman Spectra

Figure 1 and Figure 2 show the IR transmission spectra of **1** and **2** crystals. The assignments of the main characteristic IR band frequencies observed for KSeCN,[13] $Cd(SeCN)_4Zn$,[12a] **1**, and **2** are listed in Table 1. It is known that in IR spectra of the metal (M) complexes containing monodentate SeCN ligands, ν_{CN} often lies higher than 2085 cm^{-1}, ν_{CSe} lies at about 700–620 cm^{-1} (N–M bonding) or 550–500 cm^{-1} (Se–M bonding), and δ_{SeCN} lies near 425 cm^{-1} (N–M bonding) or 370 cm^{-1} (Se–M bonding).[14] From Table 1, one can see the sharp increase in frequencies of ν_{CN} stretching and ν_{CSe} stretching and the decrease in frequencies of δ_{SeCN} bending in **1** and **2** compared with the corresponding bands in the free selenocyanate radical of KSeCN. This can be explained by the electron transport model.[15] In **1** and **2** crystals, the SeCN group is a good

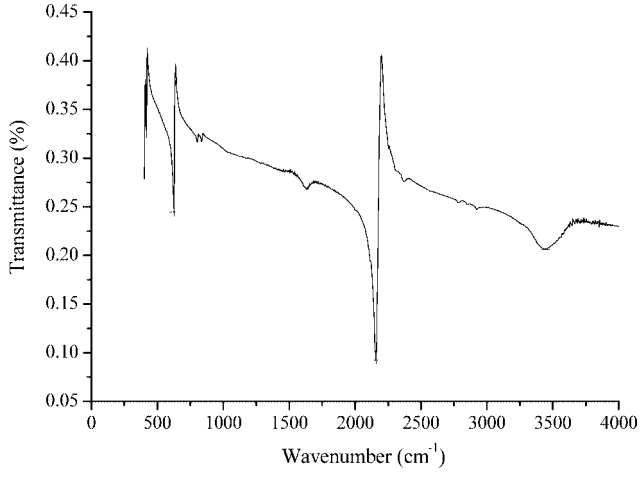

Figure 1. IR transmission spectra of **1** crystal.

electron supplier, whereas Zn^{2+}, Cd^{2+}, and Hg^{2+} are all strong electron acceptors. The electron transformation from $SeCN^-$ to Zn^{2+}, Cd^{2+}, and Hg^{2+} ions makes the wavenumbers of CN and CSe stretching vibrations increase significantly and that of SeCN bending vibrations decrease. This confirms the presence of M–N and M–Se bands in their structures.

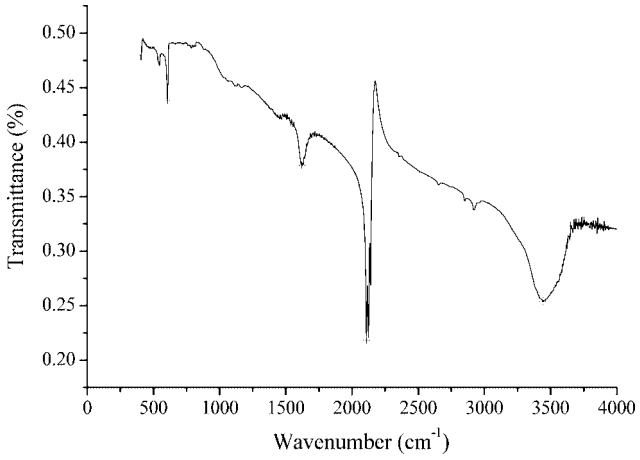

Figure 2. IR transmission spectra of **2** crystal.

Table 1. Assignments of the main characteristic IR band frequencies [cm^{-1}] observed for KSeCN,[13] $Cd(SeCN)_4Zn$,[12a] **1**, and **2**.

	KSeCN	$Cd(SeCN)_4Zn$	**1**, $[ZnCd(SeCN)_4]_n$	**2**, $[CdHg(SeCN)_4]_n$
ν_{CN}	2070	2154	2158	2140
ν_{CSe}	558	628	625	606
δ_{NCSe}	424, 416	420, 406	417, 403	407, 393

The Raman spectra (Figure 3 and Figure 4) of $AB(SeCN)_4$ (A = Zn, B = Cd for **1**; A = Cd, B = Hg for **2**), recorded at room temperature in the frequency range from 50 to 2500 cm^{-1}, consist of four frequency regions (below 100 cm^{-1}, lattice vibration modes; 100–300 cm^{-1}, vibration bands of A and B centers; 300–1200 cm^{-1}, NCSe internal vibration modes; and 2100–2200 cm^{-1}, CN stretching vibration modes). According to the vibrational spectra,[16] the Raman peaks can be assigned as ν_1 [a doubly degenerate $B(SeCN)_4$ bending vibration mode], ν_2 [a doubly degenerate $A(NCSe)_4$ bending vibration mode], ν_3 (a SeCN bending vibration mode), ν_4 (a doubly degenerate SeCN bending vibration mode), ν_5 (a CSe stretching vibration mode), and ν_6 (a CN stretching vibration mode). The Raman peaks (ν_1 and ν_2) are split on the low-wavenumber side owing to the distortion of the $B(SeCN)_4$ and $A(NCSe)_4$ tetrahedra in $AB(SeCN)_4$ crystals. The observed bands along with their vibrational assignments are summarized in Table 2.

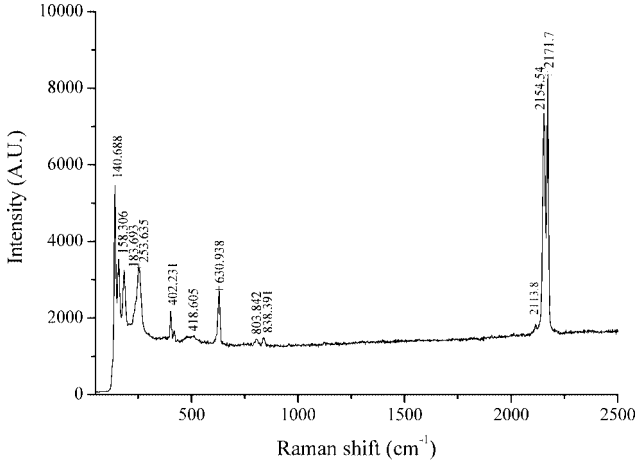

Figure 3. Raman spectra of **1** crystal.

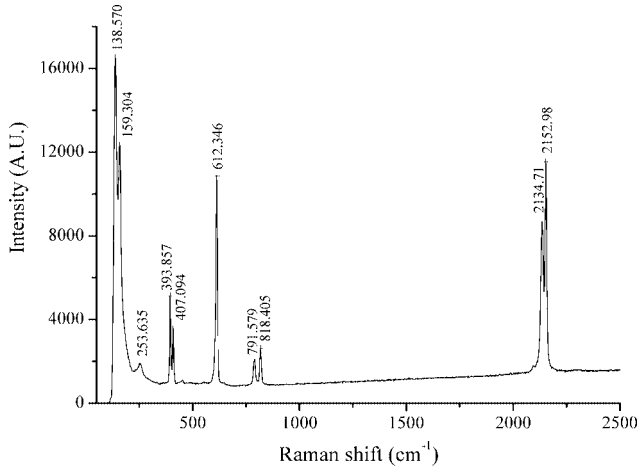

Figure 4. Raman spectra of **2** crystal.

Table 2. Assignments of the main characteristic Raman vibrational spectra data [cm^{-1}] observed for **1** and **2**.

Assignment[a]	**1**, $[ZnCd(SeCN)_4]_n$	**2**, $[CdHg(SeCN)_4]_n$
δ_{SeBSe}	141, 158, 184	138, 159
δ_{NAN}	254	253
δ_{SeCN}	402, 418	394, 407
ν_{CSe}	631	612
$2\delta_{SeCN}$	804, 838	792, 818
ν_{CN}	2114, 2155, 2172	2135, 2153

[a] A stands for Zn in **1** and for Cd in **2**; B stands for Cd in **1** and for Hg in **2**.

UV/Vis Spectra

Linear absorption spectra of **1** and **2** powders, resolved in dimethyl formamide (DMF), were determined with a 1-cm path and a concentration of 1×10^{-5} mol·dm^{-3}. The spectra show a distinctly strong absorption band at about 270 nm for **1** and 266 nm for **2**. Additionally, the solid-state electronic spectra show an intense band at approximately 263 nm for **1**, and 268 and 311 nm for **2**. These bands may be assigned to the metal-mediated ligand $\pi\rightarrow\pi^*$ charge transition of the polymeric metal–selenocyanate system. Such a transition is believed to be the origin of the NLO response.[8a]

Thermal Stability and Solubility

Thermogravimetric analyses (TGA) of **1** and **2** were performed on the single-crystal samples. The TGA curves of the two complexes exhibited that **1** was stable up to its decomposition temperature of 345.5 °C without showing any melting process and **2** did not melt until the decomposition temperature of 278.2 °C, indicating the high stability of each polymeric structure. Furthermore, in water, **1** is stable at atmospheric pressure and 65 °C for several days without decomposition and hydrolysis, while **2** decomposes and hydrolyzes if it is kept at over 45 °C for several hours.

Because of the poor solubility of **1** and **2** in common solvents, no considerably large single crystal can be grown. The experiments show that the crystals exhibit relatively high solubilities in a mixture of water and acetone (v/v = 1:3); while acetone is very volatile, they can be easily recrystallized and purified by this mixed solvent.

Description of the Structures

Some valuable experiences have been accumulated that enhance the possibility of obtaining the optimal crystallization. Single crystals obtained have low R values: polymer **1**, $R_1 = 0.0411$ and $wR_2 = 0.1058$; and polymer **2**, $R_1 = 0.0432$ and $wR_2 = 0.1031$. The latter final R indices [$I > 2\sigma(I)$] and the crystal size $0.26 \times 0.22 \times 0.14$ mm of **2** are superior to those in the related article.[12b] The crystal structures of **1** and **2** are shown in Figure 5 and Figure 6 and their molecule stackings are shown in Figure 7 and Figure 8, respectively. Crystallographic data and structure refinements for **1** and **2** are summarized in Table 3 and selected bond lengths [Å] and angles [°] are shown in Table 4.

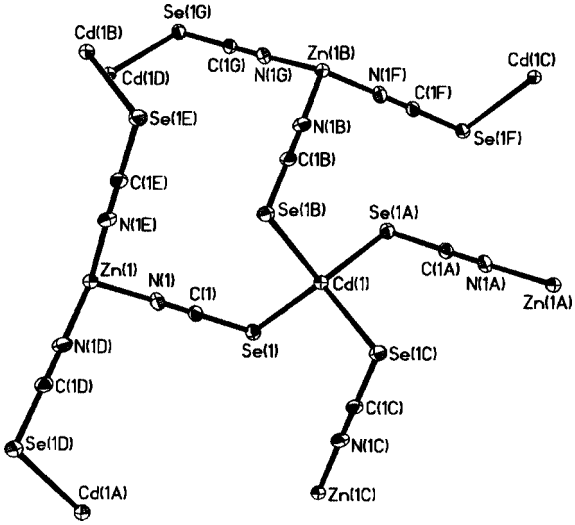

Figure 5. Crystal structure with the atom-numbering scheme of **1**.

Crystals **1** and **2** consist of two kinds of slightly flattened coordinate tetrahedrons with a local symmetry of D_{2d}: for **1** one is ZnN_4 and the other is $CdSe_4$ and for **2** one is CdN_4 and the other is $HgSe_4$. The central atoms, Zn and Cd in **1**

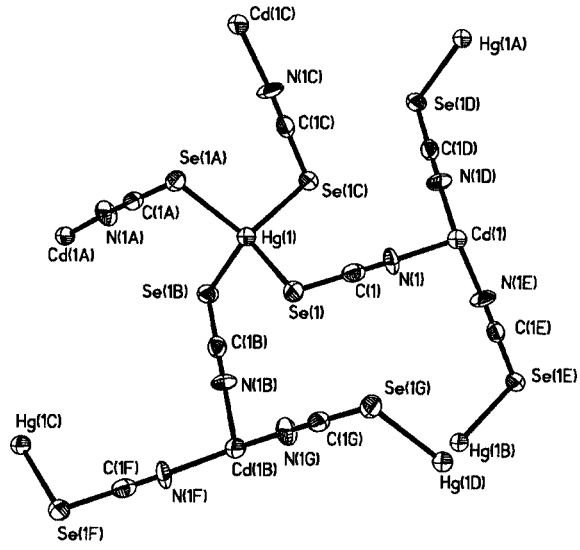

Figure 6. Crystal structure with the atom-numbering scheme of **2**.

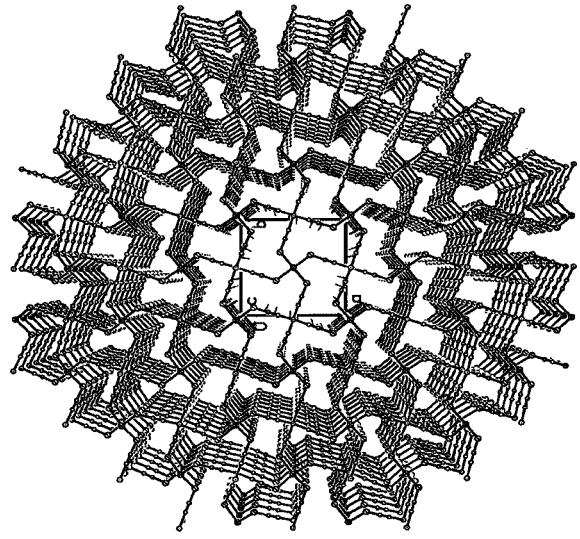

Figure 7. Molecular packing of polymer **1**.

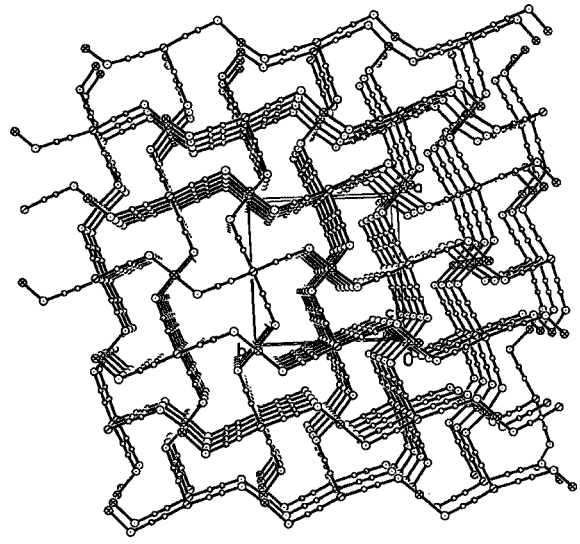

Figure 8. Molecular packing of polymer **2**.

Table 3. Crystallographic data and refinements for **1** and **2**.

Compound	**1**	**2**
Empirical formula	$C_4CdN_4Se_4Zn$	$C_4CdHgN_4Se_4$
Formula mass	597.69	732.91
Temperature [K]	293(2)	293(2)
Wavelength [Å]	0.71073	0.71073
Crystal system, space group	tetragonal, $I\bar{4}$	tetragonal, $I\bar{4}$
Unit cell dimensions [Å]	a = 11.3420(1)	a = 11.6579(7)
	c = 4.6326(1)	c = 4.5109(4)
Volume [Å^3]	595.942(15)	613.06(8)
Z, calculated density [g·cm^{-3}]	2, 3.331	2, 3.970
Absorption coefficient [mm^{-1}]	15.976	26.080
F(000)	532	632
Crystal size [mm]	0.22×0.18×0.16	0.26×0.22×0.14
Theta range for data collection [°]	$2.54 < \theta < 29.30$	$2.47 < \theta < 28.21$
Reflections collected/unique	2130/745 [R(int) = 0.0628]	2180/740 [R(int) = 0.1012]
Data/restraints/parameters	745/0/32	740/0/33
Goodness-of-fit on F^2	1.049	1.103
Final R indices [$I > 2\sigma(I)$]	R_1 = 0.0411, wR_2 = 0.1058	R_1 = 0.0432, wR_2 = 0.1031
R indices (all data)	R_1 = 0.0428, wR_2 = 0.1070	R_1 = 0.0533, wR_2 = 0.1054
Largest diff. peak and hole [e·Å^{-3}]	0.809 and –1.779	1.236 and –1.972

Table 4. Selected bond lengths [Å] and angles [°] for **1** and **2**.

1			
Cd(1)–Se(1)#1	2.6651(8)	Zn(1)–N(1)#5	1.964(8)
Cd(1)–Se(1)#2	2.6651(8)	Zn(1)–N(1)	1.964(8)
Cd(1)–Se(1)	2.6651(8)	Zn(1)–N(1)#6	1.964(8)
Cd(1)–Se(1)#3	2.6651(8)	Se(1)–C(1)	1.798(8)
Zn(1)–N(1)#4	1.964(8)	N(1)–C(1)	1.163(12)
Se(1)#1–Cd(1)–Se(1)#2	113.10(4)	N(1)#5–Zn(1)–N(1)	107.9(3)
Se(1)#1–Cd(1)–Se(1)	107.688(18)	N(1)#4–Zn(1)–N(1)#6	107.9(2)
Se(1)#2–Cd(1)–Se(1)	107.688(18)	N(1)#5–Zn(1)–N(1)#6	112.7(5)
Se(1)#1–Cd(1)–Se(1)#3	107.689(18)	N(1)–Zn(1)–N(1)#6	107.9(2)
Se(1)#2–Cd(1)–Se(1)#3	107.688(18)	C(1)–Se(1)–Cd(1)	95.1(3)
Se(1)–Cd(1)–Se(1)#3	113.10(4)	C(1)–N(1)–Zn(1)	177.6(8)
N(1)#4–Zn(1)–N(1)#5	107.9(2)	N(1)–C(1)–Se(1)	179.6(8)
N(1)#4–Zn(1)–N(1)	112.7(5)		
2			
Hg(1)–Se(1)	2.6680(13)	Cd(1)–N(1)	2.169(12)
Hg(1)–Se(1)#1	2.6680(13)	Cd(1)–N(1)#5	2.169(12)
Hg(1)–Se(1)#2	2.6680(13)	Cd(1)–N(1)#6	2.169(12)
Hg(1)–Se(1)#3	2.6680(13)	Se(1)–C(1)	1.811(15)
Cd(1)–N(1)#4	2.169(12)	N(1)–C(1)	1.140(19)
Se(1)–Hg(1)–Se(1)#1	106.91(3)	N(1)–Cd(1)–N(1)#5	112.9(9)
Se(1)–Hg(1)–Se(1)#2	114.73(6)	N(1)#4–Cd(1)–N(1)#6	112.9(9)
Se(1)#1–Hg(1)–Se(1)#2	106.91(3)	N(1)–Cd(1)–N(1)#6	107.8(5)
Se(1)–Hg(1)–Se(1)#3	106.91(3)	N(1)#5–Cd(1)–N(1)#6	107.8(4)
Se(1)#1–Hg(1)–Se(1)#3	114.73(6)	C(1)–Se(1)–Hg(1)	95.6(4)
Se(1)#2–Hg(1)–Se(1)#3	106.91(3)	C(1)–N(1)–Cd(1)	172.2(16)
N(1)#4–Cd(1)–N(1)	107.8(4)	N(1)–C(1)–Se(1)	177.1(15)
N(1)#4–Cd(1)–N(1)#5	107.8(5)		

or Hg and Cd in **2**, are located at the center of the fourfold inversion axis. From Table 4, one can see that all the Se–C–N bond angles in the two crystals are very close to 180°, that is, the SeCN group is almost perfectly linear. Therefore, the bond parameters of **1** and **2** are quite similar and it is not strange that both of them belong to the tetragonal system $I\bar{4}$ space group. Furthermore, the most striking features of the structures are the Cd–Se=C=N–Zn bridges and Hg–Se=C=N–Cd bridges, which effectively lead to the formation of an infinite three-dimensional (3D) network in a zigzag way. The coordination modes in the structures can be rationalized in terms of the hard–soft acid–base (HSAB) concept.[17]

The structural characteristics of **1** and **2** account for quite high physicochemical stability. They both possess high thermal stability and do not show hygroscopic or decomposition effects at room temperature to a great extent because of the presence of this strong polymeric structure. The asymmetric arrangements of Se and N atoms around the metal atom give rise to asymmetrical metal coordination and highly asymmetric electronic distribution about the metal atom. The extended π conjugation system within the

3D network structure, with the high polarizabilities of both the metal and the ligand, can induce desirable physical properties such as NLO effects.[8a,18]

X-ray Powder Diffraction

The X-ray powder diffraction (XRPD) patterns and diffraction indices of **1** and **2** are shown in Figure 9 and Figure 10, respectively. The tetragonal unit-cell parameters calculated by the TREOR program[19] according to the values of 2θ in the XRPD patterns are a = 11.3352, c = 4.5709 Å, V = 587.30 Å^3 for **1**, and a = 11.6450, c = 4.2155 Å, V = 571.65 Å^3 for **2**, which agree well with the results determined by the Siemens SMART CCD area detector diffractometer mentioned above.

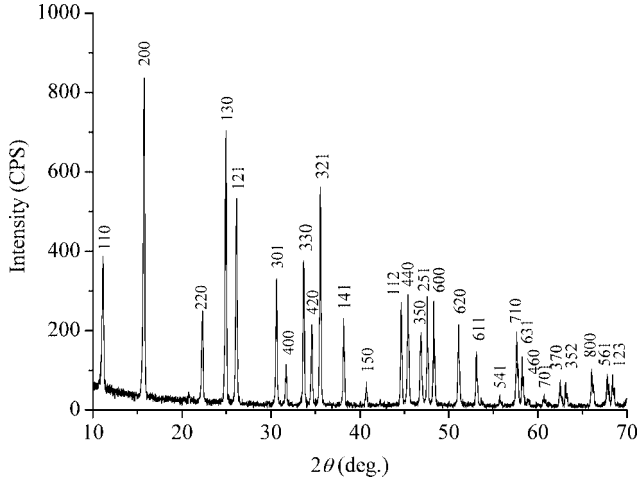

Figure 9. XRPD pattern and diffraction indices of **1** crystal.

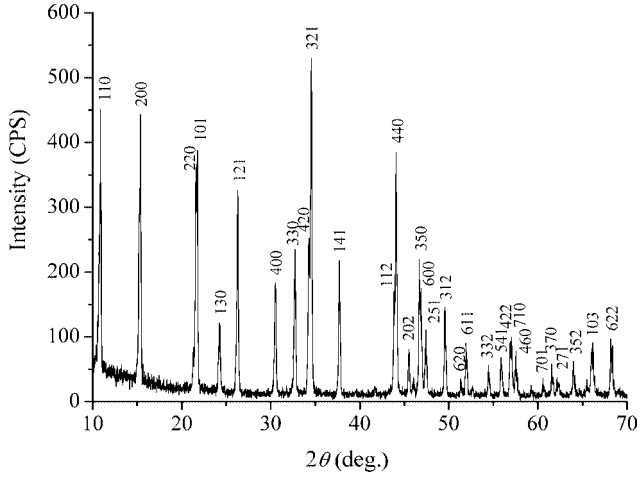

Figure 10. XRPD pattern and diffraction indices of **2** crystal.

Optical Properties

As for the feature of unsymmetrical structure, NLO activity can occur as specific physical effects. Complexes **1** and **2**, with the noncentrosymmetric space group $I\bar{4}$, were expected to give rise to efficient SHG effects for NLO application. Preliminary experimental results confirmed this and showed they both displayed strong powder SHG efficiencies. The SHG intensity was determined by the powder technique of Kurtz and Perry,[20] in which the second harmonic output was generated by irradiating powder samples of randomly oriented crystallites. The incident radiation came from a Q-switched and mode-locked Nd:YAG laser, and the results indicate that the power SHG efficiency of **1** is superior to that of **2**. The 532 nm second harmonic intensities of **1** and **2** powders were estimated as about 45 and 25 times that of NLO urea powders by direct frequency doubling of a laser diode at 1064 nm at room temperature. We assume that the high nonlinearity of the two crystals is attributed to two structural factors. One is the conjugated charge-moving bridges (Cd–Se=C=N–Zn for **1** and Hg–Se=C=N–Cd for **2**) that connect all the distorted tetrahedrons together, and the other is the effective sum of the microscopic hyperpolarizabilities originating from the parallel molecular stacking in the direction of the fourfold inversion axis. The second harmonic responses of **1** and **2** evidently resulted from the polar arrangement of all the bridging $SeCN^-$ groups, as the utilization of the asymmetric ligands can introduce electronic asymmetry, which is essential for a SHG response.[21] Considering their high thermal stability and tolerance to hydrolysis, both **1** and **2** are considered as quite promising SHG materials. Now we are managing to improving the SHG output efficiency along with exploring better crystal growth conditions.

Conclusions

The present study shows that a rational design utilizing suitable ligands and metal ions has prepared new supramolecular polymers with nonlinear optical property. The synthetic approach is based on self-assembly of the functional components into well-defined crystalline materials, which allows important structure–property relationships to be established. The title crystals possess better stability and do not show any decomposition and hygroscopic effects at room temperature, but the pH value sensitivity in solution and the physicochemical change at high temperature show the difficulties of single-crystal growth. X-ray diffraction investigations reveal that they crystallize in the same noncentrosymmetric space group, $I\bar{4}$. The high degree of polarizability of the chosen metal and the ambidentate ligand $SeCN^-$, together with the three-dimensional (3D) network structures, provide the crystals with a large interaction force between molecules, which in turn induces large macroscopic NLO properties. The SHG intensities of **1** and **2** were observed to be much stronger than that of urea powders because of the presence of distorted AN_4 (A = Zn or Cd) and BSe_4 (B = Cd or Hg) tetrahedra in the 3D structure. In summary, being 3D coordination polymers, **1** and **2** have emerged as two promising candidate materials for generation of blue-violet light using a diode laser and this, their high SHG efficiency, excellent optical transparency, and

high thermal stability make them attractive for device applications. Further studies on related properties are currently under way.

Experimental Section

General: Potassium selenocyanate (KSeCN) was prepared by the method given in the literature.[22] All other starting materials were analytical reagent grade (Purity ≥ 98.0%) and used as purchased, and all the synthetic and growth processes were carried out in aqueous solutions. Elemental analyses were performed with a Perkin–Elmer 240 instrument. IR spectra were recorded with a Nicolet FTIR 170SX instrument (KBr discs) in the 4000–400 cm^{-1} region. The far-IR spectra (500–100 cm^{-1}) were recorded in Nujol mulls between polyethylene sheets. UV/Vis spectra were recorded with a UV-265 spectrophotometer. TGA analyses were recorded with a Perkin–Elmer Pris-1 DMDA-V1 analyzer in nitrogen at a heating rate of 5 °C min^{-1}. The second-order nonlinear optical tests were carried out by the powder second harmonic generation (SHG) method.[20]

Room-temperature Raman spectra of the two crystal powders were measured on a LABRAM microscopic Raman spectrometer with a slit width of 100 nm, using a 100 mW argon ion laser at 514.53 nm with a power density of 5 mW·μm^{-2} at the sample. The Raman spectra with a resolution of 0.15 cm^{-1} and a wavelength precision of 0.5 cm^{-1} in a wavenumber range from 50 to 2500 cm^{-1} were collected.

The XRPD patterns of the **1** and **2** crystals were registered with a Rigaku D/Max-γA diffractometer, operated at 40 KV and 40 mA, using a Cu target tube and a graphite monochromator. Fixed scatter and divergence slits of 1° and a 0.15-mm receiving slit were used. The intensity data were recorded by continuous scan in a $2\theta/\theta$ mode from 10° to 70° with a step size of 0.02° and a scan speed of 4°min^{-1}.

Syntheses

$[ZnCd(SeCN)_4]_n$ (1): Cadmium chloride ($CdCl_2$) (0.03 mol, 5.50 g) was dissolved in deionized water (30 mL) at room temperature. This solution was added slowly to a colorless solution (50 mL) containing zinc chloride ($ZnCl_2$) (0.03 mol, 4.09 g) and potassium selenocyanate (KSeCN) (0.12 mol, 17.29 g). The stoichiometric mixture was stirred for 1 h and then filtered. The resulting filtrate was kept standing and evaporated slowly in a desiccator in vacuo over calcium chloride. Two weeks later, the colorless and transparent tetrahedral-shaped single crystals were obtained. Yield 12.98 g (72.4%). $ZnCd(SeCN)_4$ (597.69): calcd. C 8.03, N 9.36; found C 8.07, N 9.39.

$[CdHg(SeCN)_4]_n$ (2): This complex was prepared in an analogous way to that of **1**. Cadmium chloride ($CdCl_2$) (0.03 mol, 5.50 g) was dissolved in solution and then added slowly into a colorless solution containing mercury chloride ($HgCl_2$) (0.03 mol, 8.14 g) and potassium selenocyanate (KSeCN) (0.12 mol, 17.29 g) with stirring. After 1 h the stoichiometric mixture was filtered and evaporated slowly in a desiccator in vacuo. Twenty days later, the silvery gray and transparent tetrahedral-shaped single crystals were obtained. Yield 14.85 g (67.5%). $CdHg(SeCN)_4$ (732.91): calcd. C 6.55, N 7.64; found C 6.59, N 7.67.

Crystallographic Structure Determination: High optical quality **1** and **2** single crystals suitable for X-ray diffraction analyses were grown from their reaction mother solutions (RMS) by the solvent-evaporation method and then separated and dried, respectively. A single crystal of polymer **1** or **2** with suitable dimensions was mounted on a glass fiber and data collections were performed using a Siemens SMART CCD area detector diffractometer with Mo-K_α radiation with ω-scan mode (λ = 0.71073 Å). The structures were solved with direct methods using the program SHELXTL[23] and refined anisotropically with SHELXTL using the full-matrix least-squares procedure.

CCDC-207921 (for **1**) and -207922 (for **2**) contain the supplementary crystallographic data for this paper. These data can be obtained free of charge from The Cambridge Crystallographic Data Centre via www.ccdc.cam.ac.uk/data_request/cif.

Acknowledgments

This work was supported by the National Nature Science Foundation of China (50532030, 50335050), Doctoral Program Foundation of the Education Ministry of China, the Education Office Foundation of Anhui Province (2005KJ101), and the Malaysian Government and Universiti Sains Malaysia for the Scientific Advancement Grant Allocation (SAGA) grant No. 304/PFIZIK/653003/A118.

[1] I. Manners, *J. Polym. Sci., Part A: Polym. Chem.* **2002**, *40*, 179–191.
[2] E. Coronado, J. R. Galan-Mascaros, C. J. Gomez-Garcia, V. Laukhin, *Nature* **2000**, *408*, 447–449.
[3] A. J. Blake, N. R. Champness, P. Hubberstey, W. S. Li, M. Schröder, M. A. Withersby, *Coord. Chem. Rev.* **1999**, *183*, 117–138.
[4] P. H. Dinolfo, J. T. Hupp, *Chem. Mater.* **2001**, *13*, 3113–3125.
[5] M. Munakata, L. P. Wu, T. Kuroda-Sowa, *Adv. Inorg. Chem.* **1999**, *46*, 173–303.
[6] a) R. Kramer, I. O. Fritsky, H. Pritzkow, L. A. Kovbasyuk, *J. Chem. Soc., Dalton Trans.* **2002**, 1307–1314; b) S. Sain, T. K. Maji, G. Mostafa, T. H. Lu, M. Y. Chiang, N. R. Chaudhuri, *Polyhedron* **2002**, *21*, 2293–2299; c) K. M. Park, S. Y. Kim, J. Heo, D. Whang, S. Sakamoto, K. Yamaguchi, K. Kim, *J. Am. Chem. Soc.* **2002**, *124*, 2140–2147; d) W. J. He, F. Liu, C. Y. Duan, Z. J. Guo, S. Z. Zhou, Y. J. Liu, L. G. Zhu, *Inorg. Chem.* **2001**, *40*, 7065–7071.
[7] a) T. Bark, M. Duggeli, H. Stoeckli-Evans, A. V. Zelewsky, *Angew. Chem. Int. Ed.* **2001**, *40*, 2848–2851; b) T. W. Bell, H. Jonsselin, *Nature* **1994**, *367*, 441–444; c) W. Yeung, W. Wong, J. Zuo, T. Lau, *J. Chem. Soc., Dalton Trans.* **2000**, 629–631; d) Z. P. Zheng, *Chem. Commun.* **2001**, 2521–2529.
[8] a) H. Zhang, X. M. Wang, K. C. Zhang, B. K. Teo, *Coord. Chem. Rev.* **1999**, *183*, 157–195; b) H. Zhang, D. E. Zelmon, G. E. Price, B. K. Teo, *Inorg. Chem.* **2000**, *39*, 1868–1873; c) X. Q. Wang, D. Xu, M. K. Lu, D. R. Yuan, G. H. Zhang, F. Q. Meng, S. Y. Guo, M. Zhou, J. R. Liu, X. R. Li, *Cryst. Res. Technol.* **2001**, *36*, 73–84; d) X. Q. Wang, D. Xu, M. K. Lu, D. R. Yuan, G. H. Zhang, S. X. Xu, S. Y. Guo, X. N. Jiang, J. R. Liu, C. F. Song, Q. Ren, J. Huang, Y. P. Tian, *Mater. Res. Bull.* **2001**, *36*, 1287–1299.
[9] a) N. Zhang, M. H. Jiang, D. R. Yuan, D. Xu, X. T. Tao, Z. S. Shao, *J. Cryst. Growth* **1990**, *102*, 581–584; b) W. B. Hou, D. R. Yuan, D. Xu, N. Zhang, W. T. Yu, M. G. Liu, X. T. Tao, S. S. Ying, M. H. Jiang, *Mater. Res. Bull.* **1993**, *28*, 645–653.
[10] T. Hahn, H. Klapper, *International Tables for Crystallography*, Reidel, Dordrecht, The Netherlands, **1993**, vol. A., ch. 10.5, pp. 780–782.
[11] Y. P. Tian, S. L. Li, J. Y. Wu, S. Y. Zhang, J. X. Yang, W. Ma, "Process for the preparation of blue-violet light frequency-doubling selenocyanate complexes", CN 1440974A, September 9, **2003**; *Invention Patent Bulletin of China* (ISSN 1008-4274) **2003**, *19*, 37.

[12] a) M. Nagao, H. Inoue, S. Yanagisawa, *J. Coord. Chem.* **1980**, *10*, 29–32; b) H. Q. Sun, W. T. Yu, D. R. Yuan, X. Q. Wang, G. Xue, *Acta Crystallogr. Sect. E: Struct. Rep. Online* **2005**, *61*, i111–i112; c) Y. Y. Kharitonov, V. V. Skopenko, *Zh. Neorg. Khim.* **1965**, *10*, 1803–1805; d) G. V. Tsintsadze, V. V. Skopenko, A. E. Shvelashvili, *Soobshcheniya Akademii Nauk Gruzinskoi SSR.* **1966**, *41*, 337–340.
[13] H. W. Morgan, *J. Inorg. Nucl. Chem.* **1961**, *16*, 367–368.
[14] a) J. Chatt, L. A. Duncanson, *Nature* **1956**, *178*, 997–998; b) A. Turco, C. Pecile, M. Niccolini, *Proc. Chem. Soc. London* **1961**, 213–214; c) A. Turco, C. Pecile, M. Niccolini, *J. Chem. Soc.* **1962**, 3008–3015; d) J. L. Burmeister, Y. Al-Janabi, *Inorg. Chem.* **1965**, *4*, 962–965.
[15] K. Nakamoto, Translated by D. R. Huang, R. Q. Wang, *Infrared and Raman Spectra of Inorganic and Coordination Compounds*, 3rd ed., Chemical Industry Press, Beijing, **1986** (in Chinese).
[16] a) J. Lewis, R. S. Nyholm, P. W. Smith, *J. Chem. Soc.* **1960**, *83*, 1992–1996; b) A. Muller, K. H. Schmidt, K. H. Tytko, J. Bouwma, F. Jellinek, *Spectrochim. Acta, Part A* **1972**, *28*, 381–391; c) G. J. Kubas, L. H. Jones, *Inorg. Chem.* **1974**, *13*, 2816–2819.
[17] a) R. G. Pearson, *J. Am. Chem. Soc.* **1963**, *85*, 3533–3539; b) R. G. Pearson, *J. Am. Chem. Soc.* **1967**, *89*, 1827–1836; c) R. G. Pearson, *Science* **1966**, *151*, 172–177.
[18] J. Zyss, *Nonlinear Opt.* **1991**, *1*, 3–18.
[19] P. E. Werner, L. Eriksson, M. Westdahl, *J. Appl. Crystallogr.* **1985**, *18*, 367–370.
[20] S. K. Kurtz, T. T. Perry, *J. Appl. Phys.* **1968**, *39*, 3798–3813.
[21] a) O. R. Evans, R. G. Xiong, Z. Wang, G. K. Wong, W. Lin, *Angew. Chem. Int. Ed.* **1999**, *38*, 536–538; b) S. R. Batten, R. Robson, *Angew. Chem. Int. Ed. Engl.* **1998**, *37*, 1461–1494.
[22] G. R. Waitkins, R. Shutt, *Inorganic Synthesis*, McGraw-Hill, New York, NY, **1946**, vol. II, pp. 186–187.
[23] G. M. Sheldrick, *SHELXTL V5.1 Software Reference Manual*, Bruker AXS, Inc., Madison, WI, USA, **1997**.

Received: October 12, 2005
Published Online: May 8, 2006

